Brain Research 1651 (2016) 11–16

Contents lists available at ScienceDirect

Brain Research

journal homepage: www.elsevier.com/locate/brainres

Research report

Cerebrospinal fluid-induced retardation of amyloid β aggregation correlates with Alzheimer's disease and the *APOE* ε4 allele

E.R. Padayachee [a,*], H. Zetterberg [a,b], E. Portelius [a], J. Borén [c], J.L. Molinuevo [d], N. Andreasen [e], R. Cukalevski [f], S. Linse [f], K. Blennow [a], U. Andreasson [a]

[a] Clinical Neurochemistry Lab, Inst. of Neuroscience and Physiology, The Sahlgrenska Academy at University of Gothenburg, Mölndal, Sweden
[b] Department of Molecular Neuroscience, UCL Institute of Neurology, Queen Square, London WC1N 3BG, United Kingdom
[c] Wallenberg Laboratory, Department of Molecular and Clinical Medicine, University of Gothenburg, Gothenburg, Sweden
[d] Alzheimer's Disease and Other Cognitive Disorders Unit, Neurology Service, ICN Hospital Clinic i Universitari and Pasqual Maragall Foundation, Barcelona, Spain
[e] Department of Geriatrics, Karolinska University Hospital, Stockholm, Sweden
[f] Department of Biochemistry and Structural Biology, Lund University, Lund, Sweden

ARTICLE INFO

Article history:
Received 6 January 2016
Received in revised form
13 September 2016
Accepted 17 September 2016
Available online 23 September 2016

Keywords:
Apolipoprotein ε4
High density lipoproteins
Amyloid-β
Aggregation
Thioflavin T
Neurofibrillary tangles
Kinetics
Inhibition
Cholesterol

ABSTRACT

Misfolding and aggregation of amyloid β (Aβ) are key features of Alzheimer's disease (AD) pathogenesis, but the molecular events controlling this process are not known in detail. *In vivo*, Aβ aggregation and plaque formation occur in the interstitial fluid of the brain extracellular matrix. This fluid communicates freely with cerebrospinal fluid (CSF). Here, we examined the effect of human CSF on Aβ aggregation kinetics in relation to AD diagnosis and carrier status of the apolipoprotein E (*APOE*) ε4 allele, the main genetic risk factor for sporadic AD. The aggregation of Aβ was inhibited in the presence of CSF and, surprisingly, the effect was more pronounced in *APOE* ε4 carriers. However, by fractionation of CSF using size exclusion chromatography, it became evident that it was not the ApoE protein itself that conveyed the inhibition, since the retarding species eluted at lower volume, corresponding to a much higher molecular weight, than ApoE monomers. Cholesterol quantification and immunoblotting identified high-density lipoprotein particles in the retarding fractions, indicating that such particles may be responsible for the inhibition. These results add information to the yet unresolved puzzle on how the risk factor of *APOE* ε4 functions in AD pathogenesis.

1. Introduction

Alzheimer's disease (AD) is a devastating neurodegenerative disorder that increases with age. Given the suffering for the patients and relatives, costs for society are enormous. The neuropathological hallmarks of AD are amyloid β (Aβ) aggregates called amyloid plaques and neurofibrillary tangles consisting of hyperphosphorylated tau protein (Blennow et al., 2006). Cerebral β-amyloidosis in AD, along with findings of several causative mutations affecting Aβ production and/or aggregation in familial forms of AD, point to the significant role Aβ plays in the etiology of the disease (Glenner et al., 1984; Masters et al., 1985; Bertram and Tanzi, 2012). Aβ is produced from the amyloid precursor protein (APP; a type I transmembrane protein highly but not exclusively expressed in neurons) by sequential cleavages by β- and γ-secretase (Andreasson et al., 2012). This processing of APP releases several Aβ peptides of different lengths. Aβ1-40 is the most abundant Aβ form, whereas a 42 amino acid long, less abundant form (Aβ1-42) is the most aggregation-prone and builds up the cores of the Aβ plaques seen in AD brains (Portelius et al., 2010).

The human *APOE* gene encodes the ApoE protein which is a 299 residue apolipoprotein abundant in biological fluids and involved in the transport of lipids (Verghese et al., 2013). The gene has three alleles: *APOE* ε2, ε3 and ε4, and the translated ApoE proteins differ in sequence, structure and affinity for Aβ (Frieden and Garai, 2012; Mahley and Rall, 2000), thereby influencing the aggregation of Aβ (Strittmatter et al., 1993). The *APOE* ε4 allele is strongly associated with the sporadic late-onset AD (Corder et al., 1993; Liu et al., 2013; Poirier et al., 1993). The mechanism of this association remains unknown but seems to be intimately linked to increased risk of brain Aβ aggregation in ε4 carriers (Poirier et al., 1993).

The strong genetic link between the *APOE* ε4 allele and cerebral β-amyloidosis suggests that cholesterol may play a direct role in the pathogenesis of AD (Puglielli et al., 2003; Liu et al., 2013). Lipoprotein particles are cholesterol-rich particles produced in the

* Correspondence to: Clinical Neurochemistry Laboratory, Sahlgrenska University Hospital, House V3, S-431 80 Mölndal, Sweden.
E-mail address: padayachee.eden@gmail.com (E.R. Padayachee).

http://dx.doi.org/10.1016/j.brainres.2016.09.022

astrocytes and are found in both plasma and cerebrospinal fluid (CSF) (Ladu et al.., 1998). Lipoprotein particles are relatively high affinity Aβ binding proteins with a K_d in the nanomolar range, capable of regulating Aβ aggregation (Cole and Ard, 2000). Plasma contains three classes of lipoproteins in order of increasing size: very low density lipoproteins (VLDL), low density lipoproteins (LDL) and high density lipoproteins (HDL) (LaDu et al.., 1998). In plasma, *APOE* ε4 tends to associate with VLDL particles, and *APOE* ε3 prefers to associate with high density HDL particles (Puglielli et al., 2003). In contrast to plasma, most CSF lipoproteins are HDL-like in both density and size (Holtzman et al., 1999; Borghini et al., 1995).

In vivo, Aβ aggregation and plaque formation occur in the interstitial fluid of the brain extracellular matrix. This fluid communicates freely with CSF. Here, we examined Aβ aggregation kinetics in the presence of human CSF to test if CSF from AD patients was different from CSF from cognitively normal individuals in this regard and whether any AD-associated differences in Aβ aggregation kinetics were related to *APOE* genotype. Results from biochemical analysis of CSF fractions indicate that the factor responsible for the APOE genotype-associated effect on the aggregation kinetics of Aβ1-42 is not the ApoE protein itself but rather the HDL particles of which ApoE is a constituent.

2. Results

The formation of Aβ42 fibrils was monitored as a function of time using a highly reproducible thioflavin T fluorescence assay (Hellstrand et al., 2010; Cohen et al., 2013). The aggregation of recombinant Aβ (the full 42 amino acid sequence with an extra N-terminal methionine, which does not influence aggregation kinetics M1-42) (Walsh et al., 2009), here called Aβ42, was monitored in 20 mM Hepes/NaOH, 140 mM NaCl, 1 mM $CaCl_2$, pH 8.0 at 37 °C under quiescent condition in the presence of 10% CSF from two different cohorts (Table 1).

There was a clear retardation of Aβ42 aggregation in the presence of CSF, mainly seen as a prolonged lag phase, observed from both cohorts. Scatter plots of the resulting t½ values for samples from cohorts A and B are shown in Fig. 1. While the difference between healthy controls and AD lacking an *APOE ε4* allele was not statistically significant, the more profound retardation observed for AD patients carrying at least one *APOE ε4* allele was statistically significant ($p \leq 0.02$)..

To explore the molecular determinants behind the observed retardation, CSF was fractionated on a superose 6 size exclusion chromatography, and the aggregation kinetics was measured for Aβ42 solutions supplemented with samples from the resulting fractions. The observed aggregation curves were sigmoidal in appearance with a lag phase, a growth phase and a final plateau (Fig. 2). The half time (t½) of aggregation was extracted from each curve as the point in time where the ThT fluorescence is half-way in between the initial base line value (lag) and the final plateau

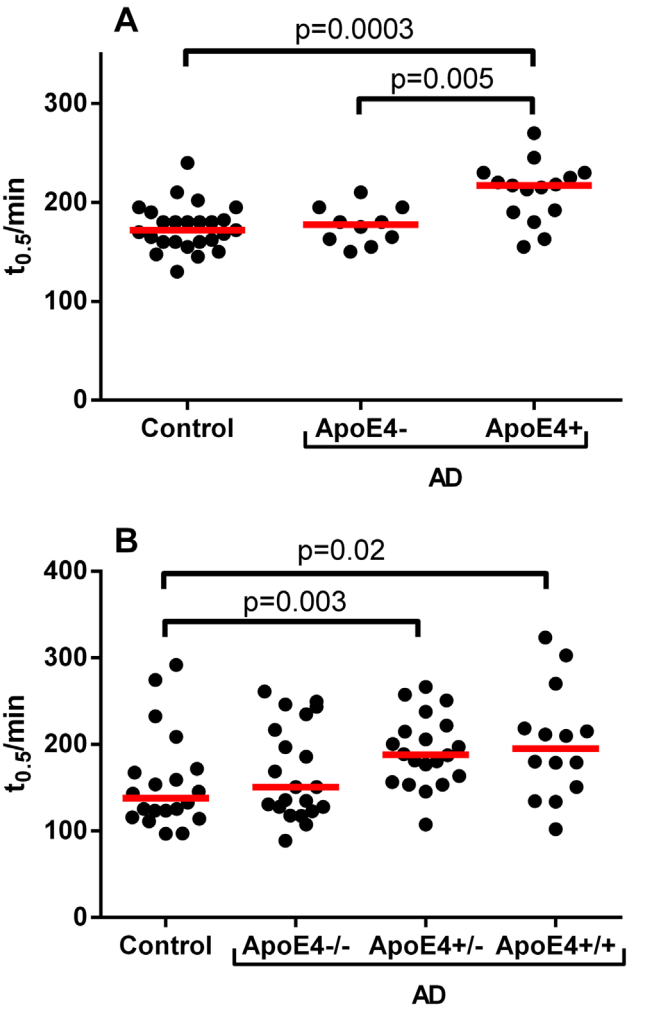

Fig. 1. Scatter plots of half time for fibril formation, t½ (mean of three replicates) for the three groups in cohort 1 (A); scatter plots of half time for fibril formation, t½ (mean of three replicates) for the four groups in cohort 2 (B).

value. Fractions 14–18, specifically fraction 15 was found to retard Aβ42 fibril formation compared to buffer, primarily observed as an extension of the lag phase (Fig. 2). Fractions 14–18 retarded Aβ42 aggregation significantly, and fraction 15 produced the longest extension of the lag phase ($t½ = 169 \pm 0.1$ min) compared to the other fractions. The cholesterol concentration was high in fractions 14–17, and the highest value (0.17 ± 0.002 mg/ml) was observed for fraction 15 (Fig. 3). Immunoblot analysis (Fig. 4) identified bands for ApoE (~36 kDa) in fractions 8–17, ApoA-I (~29 kDa) in fractions 10–18, and ApoJ (~39.8 kDa) in fractions 13–15, indicating that these fractions were rich in apolipoproteins. The bands were most intense for fraction 14–15 (ApoE), 15 (ApoA-I) and 14 (ApoJ). This finding was significant as it coincides closely

Table 1
Demographic data of two independent case-control cohorts of CSF samples obtained from Alzheimer's disease and Other Cognitive Disorders Unit, Hospital Clinic, Barcelona, Spain, and the second cohort from subjects in the Piteå Dementia Project.

	Cohort 1			Cohort 2			
	Controls	**AD**		**Controls**	**AD**		
		ApoE4 (−)	ApoE4 (+)		ApoE4 (−/−)	ApoE4 (+/−)	ApoE4 (+/+)
Number of subjects	25	10	15	20	21	20	14
Age/years mean(SD)	64.4(8.8)	68.4(7.9)	59.9(7.3)	69.8(4.4)	80.2(5.5)	76.6(7.7)	74.5(6.9)
Gender (# females)	16	8	8	10	12	11	9

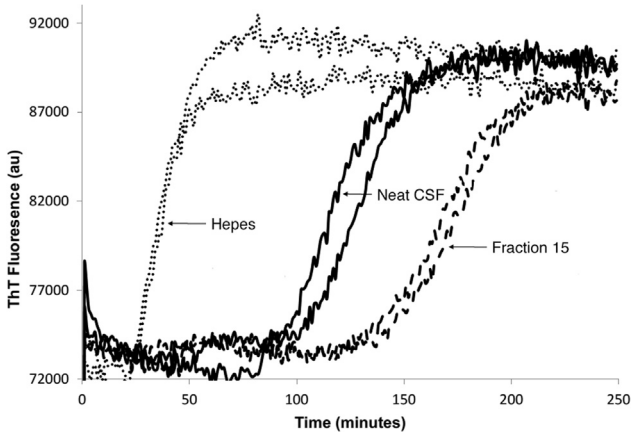

Fig. 2. Examples of sigmoidal aggregation curves monitored by Thioflavin-T fluorescence, depicting non-fractionated CSF (solid lines), a fraction after gel filtration showing the most pronounced inhibition of the kinetics (fraction 15, dashed lines). The kinetics in the absence of rate-affecting substances is within error the same as for fraction 8 (dotted lines).

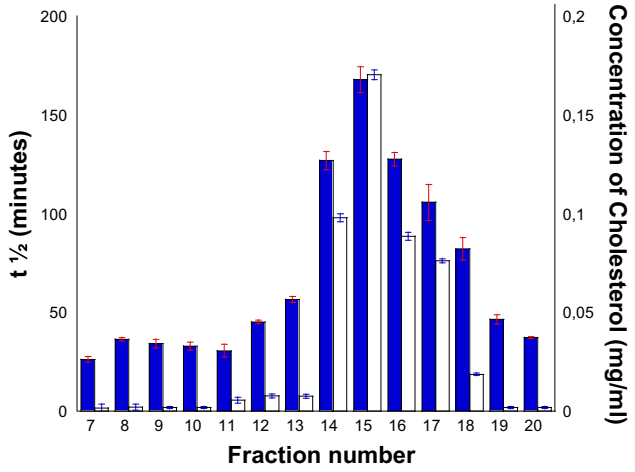

Fig. 3. A bar graph expressing t½ per a CSF fraction. Blue bars represent t½ values and white bars represent cholesterol concentration (mean of two replicates). Fraction 15 displayed the greatest t½ values of 169 min ± 0.1 min. Fraction 15 also contained the highest cholesterol concentration of 0.17 mg/ml ± 0.002 mg/ml, compared to the other fractions.

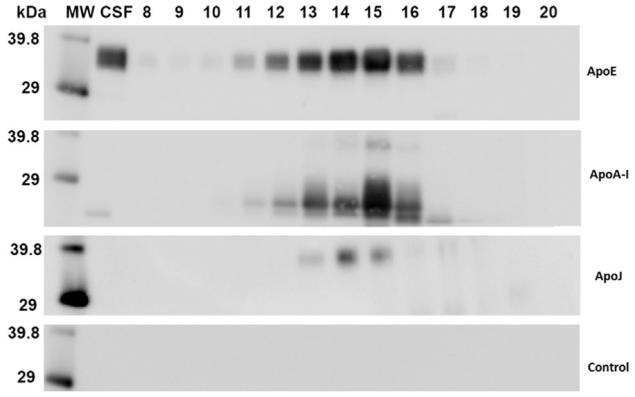

Fig. 4. Immunoblots depicting bands for ApoE (~36 kDa) (A); ApoA-I (~28 kDa) (B); ApoJ (~39.8 kDa) (C); control membrane, incubated with only with secondary antibody (D). Lane number corresponds to fraction number. The first lane marked MW is the molecular weight marker and the second lane marked CSF was the control used.

with the fractions found to delay aggregation kinetics (Fig. 3). Fractions containing lower molecular weight substances, compared to HDL complexes, were all found to have no effect on the aggregation kinetics (data not shown)....

3. Discussion

CSF was used as a surrogate matrix for brain extracellular fluid and it was found that CSF retarded Aβ aggregation in an *APOE* ε4-dependent manner. After chromatographic separation, fraction 15 influenced aggregation kinetics the most and was found to contain HDL based on cholesterol and immunoblot analyses. Our data suggest that *APOE* ε4 affects the structure of HDL or the interaction of HDL with Aβ42 to further inhibit Aβ aggregation.

Previous papers have shown that Aβ aggregation is inhibited by CSF and that the extent of inhibition is dependent on the type of *APOE* allele present (Chauhan et al., 1996; Wisniewski et al., 1993). Chauhan et al. revealed that CSF from control groups with an *APOE* ε3/3 genotype, resulted in faster Aβ aggregation than those with *APOE ε4/4* or *APOE* ε3/2 genotype. Conversely, the *APOE ε4/4* genotype was associated with a slower Aβ aggregation effect. Our current study has supported Chauhan et al., as it was observed that CSF inhibits Aβ aggregation with CSF from *APOE* ε4 carriers. Wisniewski et al.., used synthetic Aβ1-40 to examine the inhibitory effect of CSF. In the current study, we used recombinant Aβ (M1-42) to ensure that the Aβ42 preparations were not contaminated by C-terminally truncated species that are common in synthetic Aβ1-42 preparations, due to suboptimal coupling efficiency in chemical peptide synthesis and known to influence Aβ1-42 fibrillization kinetics (Finder et al., 2010).

We fractionated CSF to isolate the retarding factor and the coincidence of strongest retarding effect and elution of HDL-like particles suggest that such particles may be the component in CSF which is responsible for the Aβ inhibition effect. These particles contained apolipoproteins ApoA-I, ApoE and ApoJ that have been previously shown to bind to soluble Aβ (LaDu et al.., 1995, Koudinov et al., 1994). A similar experiment was performed by LaDu et al., using FPLC in tandem with Superose 6 columns. Western blot analysis of SDS-PAGE of selected FLPC fractions confirmed the co-localization of ApoE and Aβ to the same fractions (Ladu et al.., 2012). Normally, lipoprotein particles are separated by ultracentrifugation in potassium bromide gradients due to the density at which they float. However the high salt gradients and shear force may disturb the lipoprotein complex (Ladu et al.., 1998). Hence size exclusion chromatography was performed to preserve the native particle composition. We note however, that the retarding effect was retained also after ammonium sulfate fractionation (data not shown).

Cholesterol quantification is a commonly used method to confirm the presence of HDL particles in plasma fractions (Gustafsson et al., 2007). In our experiments, cholesterol was quantified in fractions after gel filtration and high concentrations correlated with the retardation effect. This finding, along with the immunochemical detection of several HDL-associated proteins (ApoE, ApoA and ApoJ), led us to conclude that HDL-like particles were present in these fractions and that they were responsible for retarding Aβ aggregation. It has further been shown that the ApoE- and ApoJ-containing lipoproteins are similar in size and density to plasma HDL and that ApoA-I make up 70% of the HDL particle (Fagan et al., 1999; Koudinov et al., 1996; Rached et al., 2015). Further, CSF does not contain other lipoprotein particles, such as VLDL or LDL (Otvos, 1999), which makes the association of the retarding effect of CSF on Aβ42 aggregation with HDL-like particles even stronger.

ApoE was detected in several non-retarding CSF fractions. Thus,

the retarding effect is not associated with ApoE4 itself but rather with an *APOE* ε4-associated alteration in HDL composition and/or structure. The delay in Aβ42 aggregation, with the most pronounced effect being an extension of the lag phase, has the same signature as recently observed for the chaperone DNAJ B6, which was inferred to mainly inhibit primary nucleation through interaction with nuclei or small aggregates (Mansson et al., 2014) to prevent their further growth into fibrils. While inhibition of secondary nucleation or elongation produces distinctly different effects of aggregation curves (Arosio et al., 2014; Cohen et al., 2015), the HDL-like particles seem to primarily inhibit primary nucleation. Such an effect could arise from binding of monomer, leading to lower effective concentration, or binding of nuclei or small aggregates to inhibit their further growth (Arosio et al., 2014).

The enhanced retardation observed here for *APOE* ε4 carriers may reflect their triggering of a defense mechanism to produce higher levels of HDL-like particles or more effective HDL-like particles to limit Aβ42 aggregation. Reports have also shown that *APOE* ε4 is associated with increased Aβ oligomer formation (Hashimoto et al., 2012; Garai et al., 2014). Inhibition of Aβ aggregation might result in and be consistent with increased amounts of soluble Aβ oligomers as shown in the above reports. This argument is well supported by two papers from our group, where it was stated that the toxic oligomeric species are predominantly formed from monomeric peptide molecules through a fibril-catalyzed secondary nucleation reaction (Cohen et al., 2013, 2015).

One limitation of the present study is that it was not possible to compare the effect on Aβ aggregation with respect to APOE ε4 status between controls and AD cases. However, this does not affect the interpretability of the major findings in the study.

4. Conclusion

CSF retards Aβ42 aggregation in an *APOE* ε4-dependent manner with the strongest effect observed for *APOE* ε4 carriers. The effect correlates with the concentration of HDL-like particles in size exclusion fractions of CSF, strongly suggesting HDL-like particles as the retarding factor in CSF. The kinetic signature with an extended lag phase as the most pronounced effect implies interference with primary nucleation.

5. Materials and methods

5.1. Patients

Two independent case-control cohorts of CSF samples were used in this study. Cohort 1 was prospectively recruited from the Alzheimer's disease and Other Cognitive Disorders Unit, Hospital Clinic, Barcelona, Spain, and consisted of 25 controls and 25 CE patients. Ten of the AD patients had no *APOE* ε4 allele, while 15 had at least one ε4 allele. All of the controls were *APOE* ε4 negative. The second cohort consisted of 20 healthy controls and 59 selected, based on the number of *APOE* alleles, AD cases from subjects in the Piteå Dementia Project (Andreasen et al., 1999). The AD cases comprised of 20 patients with no *APOE* ε4 allele, 20 with one *APOE* ε4 allele, and 19 with two *APOE* ε4 alleles. For the controls no *APOE* status was available. The demographics of the cohorts are shown in Table 1. All AD patients fulfilled the NINCDS-ADRDA criteria for "probable" AD according to the old criteria (Mckhann et al., 1984) for cohort 1 and the revised criteria (Mckhann et al., 2011) for cohort 2. The study was carried out in accordance with the Declaration of Helsinki.

5.2. Isolation of Aβ42 monomer and aggregation assay

Aβ (M1-42), here called Aβ42, was expressed in *E. coli* from a synthetic gene (Walsh et al., 2009). Recombinant Aβ42 was purified using ion exchange and gel filtration chromatography to generate Aβ42 monomers, which were then lyophilized and stored as dried powder at −20°C. Each day, one lyophilized Aβ42 aliquot was dissolved in 1 ml 6 M GuHCl and the monomer was isolated by gel filtration on a 1 × 30 cm Superdex 75 column in 20 mM Hepes/NaOH, 1 mM $CaCl_2$, pH 8.0. The center of monomer peak was collected in low-binding Eppendorf tube (Genuine Axygen Quality, Microtubes, MCT-200-L-C) on ice and the concentration determined from the integrated absorbance of the collected fraction of the chromatogram using ε_{280}=1400 L mol^{-1} cm^{-1}. For all CSF fractions, the Aβ42 monomer, was diluted with Hepes buffer (20 mM) containing NaCl (0.14 M) and ThT was added from a concentrated stock to obtain the final concentrations of 4 μM Aβ42 monomer and 10 μM ThT in 20 mM Hepes/NaOH, 0.14 M NaCl, 1 mM $CaCl_2$, pH 8.0. Each CSF fraction was supplemented with buffer from a concentrated stock, pH adjusted, and diluted to obtain 20% CSF in 20 mM Hepes/NaOH, 0.14 M NaCl, 1 mM $CaCl_2$, pH 8.0, and mixed 1:1 with the Aβ42 solution, so that the final samples contained 2 μM Aβ42, 6 μM ThT and 10% CSF. The final concentration of exogenous Aβ42 (2 μM=9 μg/ml) is four orders of magnitude higher than what is found in CSF (1 ng/ml), of which 10% (v/v) is present in the reaction mixture. Therefore any contribution of endogenous Aβ42 from the CSF can be neglected. The samples were mixed in low-binding tubes on ice and loaded into a black 96-well plate with clear bottom, half-area and non-binding surface (Corning 3881, Sigma Aldrich). The kinetic experiment was started by placing the plate at 37 °C in a plate reader (BMG Fluostar Omega, Optima or Galaxy). The fluorescence was read though the bottom of the plate using a 340 nm excitation filter and a 380 nm emission filter every minute for up to 350 min. The half time of aggregation ($t_{½}$) was defined as the point where the fluorescence minus initial baseline reached half the value of the equilibrium plateau and was extracted from all curves by fitting a sigmoidal function to the fluorescence intensity, y, as a function of time, t:

$$y = a + b/(1 + \exp(-(t - t_{1/2})k))$$

and plotted relative to CSF fraction number.

5.3. Fractionation of CSF by gel size exclusion chromatography

A pool of leftover, non-traceable CSF samples (40 ml) from clinical routine analysis of normal (*i.e.* non-AD) patients was centrifuged at 2250 × *g* for 10 min at room temperature (25 °C). The supernatant was transferred by pipetting. After continuous mixing, 1 ml was aliquoted and frozen at −20 °C. Centrifuged CSF (4 ml) was concentrated using an amicon filter (10 kDa MWCO) and 0.2 ml of the concentrate was applied independently to Superose 6 10/300 GL column. All protein fractions were eluted with isocratic PBS buffer (0.14 M NaCl, 0.0027 M KCl and 0.010 M phosphate, pH 7.4); flow rate 0.5 ml/min, 1 ml fractions). All fractions from CSF were stored at −20 °C and tested against the ThT kinetic assay.

5.4. Cholesterol analysis

Cholesterol was quantified in all fractions from gel exclusion chromatography, using commercially available kits (Cholesterol Infinity Kit, Thermofisher). The cholesterol standard was MCC Cal 2 (Abbott Laboratories, USA), which contained 10.05 mM cholesterol. Each fraction, standard and blank (PBS), respectively, was

pipetted (20 μl) into a 96 well plate. The Infinity™ Cholesterol Liquid Stable reagent (100 μl) was added to the wells and mixed well (15x) on the ELISA plate reader at 37 °C for 15 min. Absorbance was recorded at 500 nm and 660 nm in the ELISA plate reader. Readings at 660 nm were subtracted from readings at 500 nm to correct for optical imperfections in the plate.

5.5. Immunoblotting

Biotinylated molecular weight marker (Sigma Aldrich, Cat No. B2787) was diluted 1:20 in 1 × Nu-PAGE LDS sample buffer (without DTT). CSF not subjected to size exclusion chromatography was used as positive control and incubation of membrane with no primary antibody was used as negative control. Fractions 8–20 from size exclusion chromatography were diluted 2 × with Nu-PAGE LDS sample buffer containing 0.5 M DTT. Undiluted CSF fractions were tested against the ApoJ antibody. The molecular weight marker, along with all fractions, including CSF, were separated by electrophoresis in NU-PAGE 10% Bis-Tris gels (Invitrogen Corporation) using the Nu-PAGE mini-gel system (Xcell II Mini-Cell [Novex, San Diego, CA, USA]). The proteins were transferred (0.7 mA/cm2) to Immobilon PVDF membranes (Millipore Corporation, Billerica, MA, USA) using the semi-dry blotting technique (Trans-Blot semi-dry Transfer cell). Blocking was performed for 1 h at room temperature (RT) using 5% dry milk powder in PBS-T (0.05% v/v Tween 20) (Blocking grade blocker, Non-Fat dry milk, Bio-Rad Laboratories, USA). Incubations with the primary antibodies (diluted 1:2000 in 5% dry milk) were performed overnight at +4 °C. The following primary antibodies were used to monitor the presence of lipoproteins in CSF: monoclonal mouse anti-human apolipoprotein E antibody; monoclonal mouse anti-human apolipoprotein A1 antibody; monoclonal mouse anti-human apolipoprotein J/Clusterin antibody (Novus Biologicals, Europe). The membranes were washed for 6 × 10 min in PBS-T (PBS with 0.05% v/v Tween 20) and then incubated for 1 h at room temperature (RT) with biotinylated anti-mouse IgG antibody (Vector Laboratories, Burlingame, CA, USA) (1 mg/ml), diluted 1:3000 in PBS-T. A second PBS-T wash was performed for 6 × 10 min after which the membranes were incubated for 1 h at RT with streptavidin-biotinylated horseradish peroxidase complex (GE Healthcare UK Limited, Buckinghamshire, UK) diluted 1:3000 in PBS-T. Following 6 × 10 min washes, the membranes were developed for 2 min with Amersham ECL select Immunoblot detection reagent (GE Healthcare) solution according to the manufacturer's instructions. The emitted signal was detected by a Fujifilm LAS-3000 System (FUJIFILM Corporation).

Acknowledgments

The authors wish to thank the European Medical Information Framework for financial assistance.

References

Andreasen, N., Blennow, K., Sjodin, C., Winblad, B., Svardsudd, K., 1999. Prevalence and incidence of clinically diagnosed memory impairments in a geographically defined general population in Sweden. The Pitea Dementia Project. Neuroepidemiology 18, 144–155.

Andreasson, U., Vanmechelen, E., Shaw, L.M., Zetterberg, H., Vanderstichele, H., 2012. Analytical aspects of molecular Alzheimer's disease biomarkers. Biomark. Med. 6, 377–389.

Arosio, P., Vendruscolo, M., Dobson, C.M., Knowles, T.P., 2014. Chemical kinetics for drug discovery to combat protein aggregation diseases. Trends Pharm. Sci. 35, 127–135.

Bertram, L., Tanzi, R.E., 2012. The genetics of Alzheimer's disease. Prog. Mol. Biol. Transl. Sci. 107, 79–100.

Blennow, K., De Leon, M.J., Zetterberg, H., 2006. Alzheimer's disease. Lancet 368, 387–403.

Borghini, I., Barja, F., Pometta, D., James, R.W., 1995. Characterization of subpopulations of lipoprotein particles isolated from human cerebrospinal fluid. Biochim. Biophys. Acta 1255, 192–200.

Chauhan, A., Pirttila, T., Mehta, P., Chauhan, V.P., Wisniewski, H.M., 1996. Effect of cerebrospinal fluid from normal and Alzheimer's patients with different apolipoprotein E phenotypes on in vitro aggregation of amyloid beta-protein. J. Neurol. Sci. 141, 54–58.

Cohen, S.I., Arosio, P., Presto, J., Kurudenkandy, F.R., Biverstal, H., Dolfe, L., Dunning, C., Yang, X., Frohm, B., Vendruscolo, M., Johansson, J., Dobson, C.M., Fisahn, A., Knowles, T.P., Linse, S., 2015. A molecular chaperone breaks the catalytic cycle that generates toxic Abeta oligomers. Nat. Struct. Mol. Biol. 22, 207–213.

Cohen, S.I., Linse, S., Luheshi, L.M., Hellstrand, E., White, D.A., Rajah, L., Otzen, D.E., Vendruscolo, M., Dobson, C.M., Knowles, T.P., 2013. Proliferation of amyloid-beta42 aggregates occurs through a secondary nucleation mechanism. Proc. Natl. Acad. Sci. USA 110, 9758–9763.

Cole, G.M., Ard, M.D., 2000. Influence of lipoproteins on microglial degradation of Alzheimer's amyloid beta-protein. Microsc. Res. Tech. 50, 316–324.

Corder, E.H., Saunders, A.M., Strittmatter, W.J., Schmechel, D.E., Gaskell, P.C., Small, G.W., Roses, A.D., Haines, J.L., Pericak-Vance, M.A., 1993. Gene dose of apolipoprotein E type 4 allele and the risk of Alzheimer's disease in late onset families. Science 261, 921–923.

Fagan, A.M., Holtzman, D.M., Munson, G., Mathur, T., Schneider, D., Chang, L.K., Getz, G.S., Reardon, C.A., Lukens, J., Shah, J.A., Ladu, M.J., 1999. Unique lipoproteins secreted by primary astrocytes from wild type, apoE (-/-), and human apoE transgenic mice. J. Biol. Chem. 274, 30001–30007.

Finder, V.H., Vodopivec, I., Nitsch, R.M., Glockshuber, R., 2010. The recombinant amyloid-beta peptide Abeta1-42 aggregates faster and is more neurotoxic than synthetic Abeta1-42. J. Mol. Biol. 396, 9–18.

Frieden, C., Garai, K., 2012. Structural differences between apoE3 and apoE4 may be useful in developing therapeutic agents for Alzheimer's disease. Proc. Natl. Acad. Sci. USA 109, 8913–8918.

Garai, K., Verghese, P.B., Baban, B., Holtzman, D.M., Frieden, C., 2014. The binding of apolipoprotein E to oligomers and fibrils of amyloid-beta alters the kinetics of amyloid aggregation. Biochemistry 53, 6323–6331.

Glenner, G.G., Wong, C.W., Quaranta, V., Eanes, E.D., 1984. The amyloid deposits in Alzheimer's disease: their nature and pathogenesis. Appl. Pathol. 2, 357–369.

Gustafsson, M., Levin, M., Skalen, K., Perman, J., Friden, V., Jirholt, P., Olofsson, S.O., Fazio, S., Linton, M.F., Semenkovich, C.F., Olivecrona, G., Boren, J., 2007. Retention of low-density lipoprotein in atherosclerotic lesions of the mouse: evidence for a role of lipoprotein lipase. Circ. Res. 101, 777–783.

Hashimoto, T., Serrano-Pozo, A., Hori, Y., Adams, K.W., Takeda, S., Banerji, A.O., Mitani, A., Joyner, D., Thyssen, D.H., Bacskai, B.J., Frosch, M.P., Spires-Jones, T.L., Finn, M.B., Holtzman, D.M., Hyman, B.T., 2012. Apolipoprotein E, especially apolipoprotein E4, increases the oligomerization of amyloid beta peptide. J. Neurosci. 32, 15181–15192.

Hellstrand, E., Boland, B., Walsh, D.M., Linse, S., 2010. Amyloid beta-protein aggregation produces highly reproducible kinetic data and occurs by a two-phase process. ACS Chem. Neurosci. 1, 13–18.

Holtzman, D.M., Bales, K.R., Wu, S., Bhat, P., Parsadanian, M., Fagan, A.M., Chang, L. K., Sun, Y., Paul, S.M., 1999. Expression of human apolipoprotein E reduces amyloid-beta deposition in a mouse model of Alzheimer's disease. J. Clin. Investig. 103, R15–R21.

Koudinov, A., Matsubara, E., Frangione, B., Ghiso, J., 1994. The soluble form of Alzheimer's amyloid beta protein is complexed to high density lipoprotein 3 and very high density lipoprotein in normal human plasma. Biochem. Biophys. Res. Commun. 205, 1164–1171.

Koudinov, A.R., Koudinova, N.V., Kumar, A., Beavis, R.C., Ghiso, J., 1996. Biochemical characterization of Alzheimer's soluble amyloid beta protein in human cerebrospinal fluid: association with high density lipoproteins. Biochem. Biophys. Res. Commun. 223, 592–597.

Ladu, M.J., Gilligan, S.M., Lukens, J.R., Cabana, V.G., Reardon, C.A., Van Eldik, L.J., Holtzman, D.M., 1998. Nascent astrocyte particles differ from lipoproteins in CSF. J. Neurochem. 70, 2070–2081.

Ladu, M.J., Pederson, T.M., Frail, D.E., Reardon, C.A., Getz, G.S., Falduto, M.T., 1995. Purification of apolipoprotein E attenuates isoform-specific binding to beta-amyloid. J. Biol. Chem. 270, 9039–9042.

Ladu, M.J., Munson, G.W., Jungbauer, L., Getz, G.S., Reardon, C.A., Tai, L.M., Yua, C., 2012. Preferential interactions between ApoE-containing lipoprotiens and Aβ revealed by a detection method that combines size exclusion chromatography with non-reducing gel-shift. Biochim. Biophys. Acta 1821, 295–302.

Liu, C.C., Kanekiyo, T., Xu, H., Bu, G., 2013. Apolipoprotein E and Alzheimer disease: risk, mechanisms and therapy. Nat. Rev. Neurol. 9, 106–118.

Mahley, R.W., Rall, S.C.,J.R., 2000. Apolipoprotein E: far more than a lipid transport protein. Annu. Rev. Genom. Hum. Genet. 1, 507–537.

Mansson, C., Arosio, P., Hussein, R., Kampinga, H.H., Hashem, R.M., Boelens, W.C., Dobson, C.M., Knowles, T.P., Linse, S., Emanuelsson, C., 2014. Interaction of the molecular chaperone DNAJB6 with growing amyloid-beta 42 (Abeta42) aggregates leads to sub-stoichiometric inhibition of amyloid formation. J. Biol. Chem. 289, 31066–31076.

Masters, C.L., Simms, G., Weinman, N.A., Multhaup, G., Mcdonald, B.L., Beyreuther, K., 1985. Amyloid plaque core protein in Alzheimer disease and Down syndrome. Proc. Natl. Acad. Sci. USA 82, 4245–4249.

Mckhann, G., Drachman, D., Folstein, M., Katzman, R., Price, D., Stadlan, E.M., 1984. Clinical diagnosis of Alzheimer's disease: report of the NINCDS-ADRDA Work

group under the auspices of department of health and human services task force on Alzheimer's disease. Neurology 34, 939–944.
Mckhann, G.M., Knopman, D.S., Chertkow, H., Hyman, B.T., Jack, C.R., Kawas, J.R., Klunk, C.H., Koroshetz, W.E., Manly, W.J., Mayeux, J.J., Mohs, R., Morris, R.C., Rossor, J.C., Scheltens, M.N., Carrillo, P., Thies, M.C., Weintraub, S, B., Phelps, C. H., 2011. The diagnosis of dementia due to Alzheimer's disease: recommendations from the national institute on aging-Alzheimer's association workgroups on diagnostic guidelines for Alzheimer's disease. Alzheimers Dement. 7, 263–269.
Otvos, J., 1999. Measurement of triglyceride-rich lipoproteins by nuclear magnetic resonance spectroscopy. Clin. Cardiol. 22, II21–II27.
Poirier, J., Davignon, J., Bouthillier, D., Kogan, S., Bertrand, P., Gauthier, S., 1993. Apolipoprotein E polymorphism and Alzheimer's disease. Lancet 342, 697–699.
Portelius, E., Bogdanovic, N., Gustavsson, M.K., Volkmann, I., Brinkmalm, G., Zetterberg, H., Winblad, B., Blennow, K., 2010. Mass spectrometric characterization of brain amyloid beta isoform signatures in familial and sporadic Alzheimer's disease. Acta Neuropathol. 120, 185–193.
Puglielli, L., Tanzi, R.E., Kovacs, D.M., 2003. Alzheimer's disease: the cholesterol connection. Nat. Neurosci. 6, 345–351.
Rached, F.H., Chapman, M.J., Kontush, A., 2015. HDL particle subpopulations: focus on biological function. Biofactors 41, 67–77.
Strittmatter, W.J., Saunders, A.M., Schmechel, D., Pericak-Vance, M., Enghild, J., Salvesen, G.S., Roses, A.D., 1993. Apolipoprotein E: high-avidity binding to beta-amyloid and increased frequency of type 4 allele in late-onset familial Alzheimer disease. Proc. Natl. Acad. Sci. USA 90, 1977–1981.
Walsh, D.M., Thulin, E., Minogue, A.M., Gustavsson, N., Pang, E., Teplow, D.B., Linse, S., 2009. A facile method for expression and purification of the Alzheimer's disease-associated amyloid beta-peptide. FEBS J. 276, 1266–1281.
Verghese, P.B., Castellano, J.M., Garai, K., Wang, Y., Jiang, H., Shah, A., Bu, G., Frieden, C., Holtzman, D.M., 2013. ApoE influences amyloid-beta (Abeta) clearance despite minimal apoE/Abeta association in physiological conditions. Proc. Natl. Acad. Sci. USA 110, E1807–E1816.
Wisniewski, T., Castano, E., Ghiso, J., Frangione, B., 1993. Cerebrospinal fluid inhibits Alzheimer beta-amyloid fibril formation in vitro. Ann. Neurol. 34, 631–633.